

CONF-960848-13

Monochromators for small cross-section x-ray beams from high heat flux
synchrotron sources

Gene Ice and Bernie Riemer

Metals and Ceramics Division, Oak Ridge National Laboratory
Oak Ridge TN 38931-6118

Ali Khounsary

Advanced Photon Source, Experimental Facilities Division
Argonne National Laboratory, 9700 S. Cass Avenue, Argonne IL 60439

RECEIVED

SEP 13 1996

OSTI

ABSTRACT

For some x-ray experiments, only a fraction of the intense central cone of x-rays generated by high-power undulator sources can be used; the x-ray source emittance is larger than the useful emittance for the experiment. For example with microfocusing optics, or for coherence experiments, x-ray beams with cross sections less than 0.1 mm^2 are desirable. With such small beams, the total thermal load is small even though the heat flux density is high. Analyses indicate that under these conditions, rather simple crystal cooling techniques can be used. We illustrate the advantages of a small beam monochromator, with a simple x-ray monochromator optimized for x-ray microdiffraction. This monochromator is designed to achieve negligible distortion when subjected to a narrow (0.1 mm wide) beam from an APS undulator A operating at 100 mA. It also allows for rapid and repeatable energy scans and rapid cycling between monochromatic and white beam conditions.

1. INTRODUCTION

Insertion devices on third generation synchrotron sources provide ultra-brilliant ($\text{p/s} \cdot \mu\text{m}^2 \cdot \text{mrad}^2 \cdot \text{eV}$) x-ray beams with kilowatts of x-ray power into a small solid angle (Fig. 1). These intense x-ray beams challenge conventional x-ray monochromator optics and have led to the development of new high heat-load monochromators.¹⁻³ X-ray monochromators proposed for handling undulator radiation from 3rd generation x-ray sources include, inclined Si crystals¹, diamond crystals², and cryogenically cooled Si.³ These monochromators are designed to preserve x-ray flux while accepting hundreds of watts of power in the bright central cone of undulator radiation.

Although these new designs are useful for many experiments, they can be inefficient for experiments where maximum beam brilliance is required in a very small beam emittance. For example, the bandpass of diamond crystals is about half that of Si, and it is difficult to get perfect diamond crystals with negligible mosaic spread. Similarly, inclined crystals are difficult to fabricate with negligible strain, and increase the required beam offset compared to symmetric Bragg geometries. With cryogenic Si monochromators, existing first crystal designs preclude small offsets and exhibit residual stresses from the cryogenic cooling manifold. For experiments which can use only a small fraction of the beam central cone, the total useful power can be 1-3 orders of magnitude lower than for conventional experiments (Fig. 1). This allows much simpler first crystals which tolerate high power density but only work with small integrated power loads.

DISTRIBUTION OF THIS DOCUMENT IS UNLIMITED

MASTER

The submitted manuscript has been authored by a contractor of the U.S. Government under contract No. DE-AC05-96OR22464. Accordingly, the U.S. Government retains a nonexclusive, royalty-free license to publish or reproduce the published form of this contribution, or allow others to do so, for U.S. Government purposes.

DISCLAIMER

**Portions of this document may be illegible
in electronic image products. Images are
produced from the best available original
document.**

DISCLAIMER

This report was prepared as an account of work sponsored by an agency of the United States Government. Neither the United States Government nor any agency thereof, nor any of their employees, makes any warranty, express or implied, or assumes any legal liability or responsibility for the accuracy, completeness, or usefulness of any information, apparatus, product, or process disclosed, or represents that its use would not infringe privately owned rights. Reference herein to any specific commercial product, process, or service by trade name, trademark, manufacturer, or otherwise does not necessarily constitute or imply its endorsement, recommendation, or favoring by the United States Government or any agency thereof. The views and opinions of authors expressed herein do not necessarily state or reflect those of the United States Government or any agency thereof.

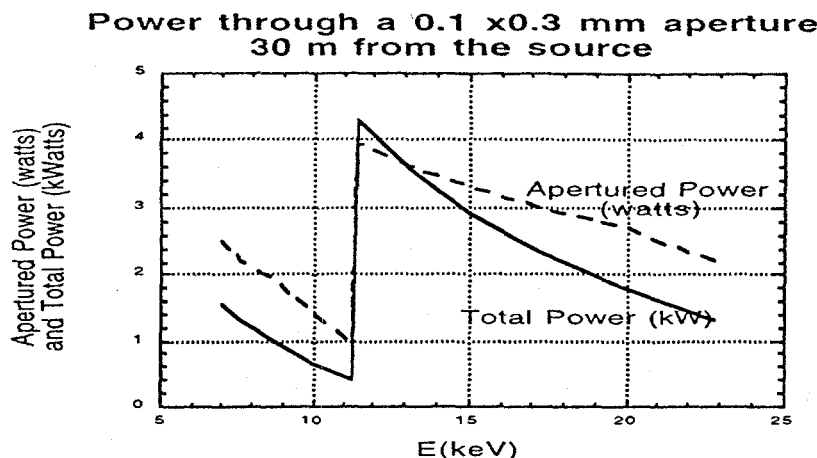


Fig. 1. Power through a 0.1×0.3 mm aperture (solid line) compared to the total power in a type A undulator at the APS (dashed line). Below 10 keV highest brilliance comes from the first harmonic and above 10 keV highest brilliance comes from the third harmonic.

Both x-ray microdiffraction and x-ray coherent diffraction are classes of experiments where beam brilliance represents the critical figure of merit and where the useful beam emittance is much smaller than the natural beam emittance from an undulator. For x-ray microdiffraction, the useful beam emittance is set by requirements for spatial resolution and momentum transfer resolution. In both the horizontal and vertical directions, only about 1 nm rad can be accepted by ideal optics; beam brilliance within this emittance establishes the achievable microdiffraction performance. For coherent diffraction only about 0.1 nm rad of beam emittance can be used. As shown in Fig 2, the vertical emittance from an APS undulator A with 2% coupling is well matched to the useable emittance for x-ray microdiffraction but large compared to the useable emittance for coherent diffraction. The horizontal emittance from a type A undulator is very large compared to the useable emittance for both x-ray microdiffraction and x-ray coherent diffraction.

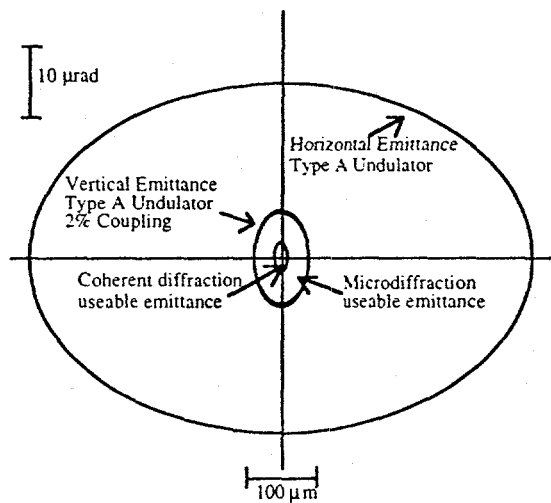


Fig. 2 Vertical and horizontal phase space ellipses at ~ 10 keV for an APS type A undulator with 2% coupling compared to the useable emittance for various experiments. The vertical emittance is well matched to the useable emittance for x-ray microdiffraction, but is large compared to the useable emittance for coherent diffraction. The horizontal emittance from a type A undulator is very large compared to both the useable emittance for x-ray microdiffraction and x-ray coherent diffraction.

The root-mean-square, RMS, divergence of an undulator power distribution is $\sim 1/\gamma$ in the vertical plane and $\sim K/\gamma$ in the horizontal plane. Here γ is related to the ring energy E by $\gamma = 1957E(\text{keV})$. Assuming a Gaussian power distribution with $K \sim 1$, the power in a small central spot of dimensions Δx and Δy is given by,

$$dP = \frac{P_T \Delta x \Delta y \gamma^2}{2\pi F_1^2}. \quad (1)$$

Here F_1 is the distance from the aperture to the source and P_T is the total beam power. For microdiffraction optics at $F_1 = 30\text{m}$, only about a 0.3mm high by 0.1mm wide beam can be efficiently collected and focused to submicron dimensions.⁴ The power through a defining slit of $0.1\text{mm} \times 0.3\text{mm}$ is about three orders of magnitude less than the total beam power and is an order of magnitude less than commonly experienced by 2nd generation x-ray optics. However, the power density is still very high.

To check this rough estimate and to help in more detailed modeling, we estimate the power through a $0.1\text{mm} \times 0.3\text{mm}$ aperture with the program Urgent. A type A undulator was assumed with 100 mA beam current and 7 GeV operations. The total power through a $0.1 \times 0.3\text{ mm}$ aperture was calculated with the undulator optimized for highest on-axis brilliance for $8\text{-}25\text{ keV}$ x-rays. The estimated total power in the beam is shown as a dotted line in Fig. 1. The total power through the aperture, integrated from 3 to 90 keV , is shown as the solid line in Fig. 1. As illustrated, the power through the aperture is about 1000 times less than in the total undulator beam and varies between $1\text{-}4$ watts, when the undulator is optimized for maximum brilliance from 8 keV to 25 keV . The power can be slightly reduced above 10 keV by the use of low Z filters to eliminate the first harmonic from the undulator spectra.

Below we describe a simple x-ray monochromator optimized for x-ray microdiffraction where the incident beam on the sample can be rapidly switched between monochromatic and "white" beam conditions. The beam offset is minimized to simplify the effects on the beam focus when the beam is switched between white and monochromatic conditions. Several alternative designs and the relative advantages and disadvantages are discussed.

2. SMALL DISPLACEMENT MONOCHROMATOR DESIGNS

2-Crystal Design

The challenge of x-ray microdiffraction is to determine the crystallographic structure of the sample, while illuminating a small volume of material. In some cases it is possible to use large beams and illuminate small isolated crystals. Here traditional x-ray diffraction techniques which involve rotating the sample are appropriate. For many samples however, it is their small volume inhomogeneity within large volumes which is of greatest interest. Here small x-ray probes are used to characterize the structure on a micron scale. With non-homogeneous samples, traditional rotation methods are difficult because the sphere of uncertainty for most diffractometers is finite and because the volume of the illuminated sample changes as the sample orientation is changed. Fig. 3 illustrates how the volume irradiated changes on rotation and depends on the distance of the center of rotation from the point of beam penetration.

One method which can be used to measure structure without rotating the sample is white beam Laue diffraction. This method takes advantage of the tunability of synchrotron radiation and avoids many problems associated with monochromatic diffraction methods, since the volume of sample illuminated remains fixed during the measurement. With the white beam Laue method, the sample is positioned relative to a small x-ray probe beam with an x-y-z stage. The sample orientation remains fixed while a broad bandpass x-ray beam illuminates the sample. Laue spots provide information about the phase, orientation

and all the average unit cell parameters except the unit cell volume. In polycrystalline samples, there will be Laue patterns superimposed from all the grains illuminated by the x-ray microbeam.

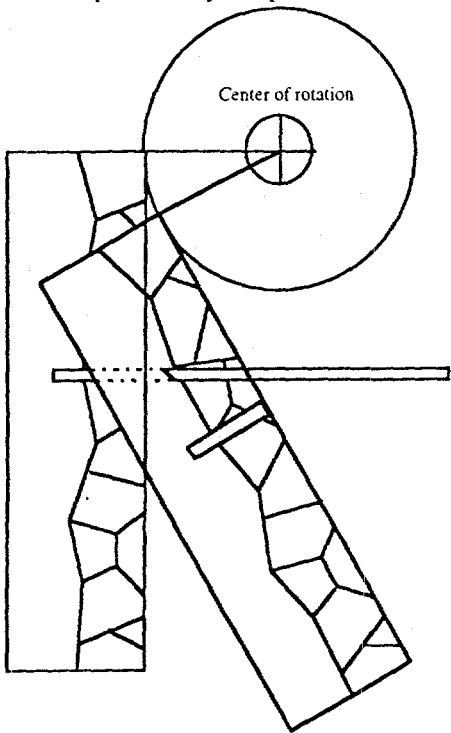


Fig. 3. The microstructure (shown here as surface grains) which intercepts the x-ray probe beam, changes as the angle of the sample is rotated. Even if the sample is perfectly aligned relative to the rotation axes, the finite penetration ensures that a different volume is illuminated as the sample is rotated.

To determine the unit cell volume of each grain, the energy of a single Laue reflection from each grain is measured. This can be done by using a solid state detector^{5,6} or crystal analyzer to measure the energy of a Laue spot, or by inserting a monochromator into the direct beam and scanning the incident energy to determine the x-ray energy needed for the Laue spot⁷. Energy resolution of 1 part in 10^4 is needed for many measurements.

Because the x-ray beams required for x-ray microprobe experiments are small, it is possible to consider the development of an ultra-small displacement monochromator design for the incident beam monochromator. This has a major advantage for x-ray microprobe experiments since it allows the focusing optics to remain nearly fixed while the focused beam is cycled between white and monochromatic conditions. Consider for example Fig. 4 which illustrates an ~2 mm high central cone from an x-ray undulator, which impinges on a small displacement x-ray monochromator. With a small displacement of the beam (~1 mm), it is possible to maintain a fixed exit with either monochromatic or white radiation and still remain near the central bright region of the undulator.

Although the design illustrated in Fig. 4 ensures that the beam exits from the same vertical aperture both with or without the monochromator, there is a small angular difference between the monochromatic and white beams which exit from the final aperture. A 1 mm displacement at 30 m for example, corresponds to an angular change of 0.03 mrad. With a 100:1 vertical demagnification this will result in a displacement of the beam by ~10 μ m and an increased effective source size of 10% due to the change in the projected source size. The displacement can be corrected with a small angular tilt of the first mirror. This angular tilt will result in a small (of order 0.5%) change in the focal length with about a 14% blurring of the x-ray beam spot. In most cases imperfections in the mirror system will limit the achievable demagnification for a given focal length so this additional blurring should have only a very small effect on the final image size.

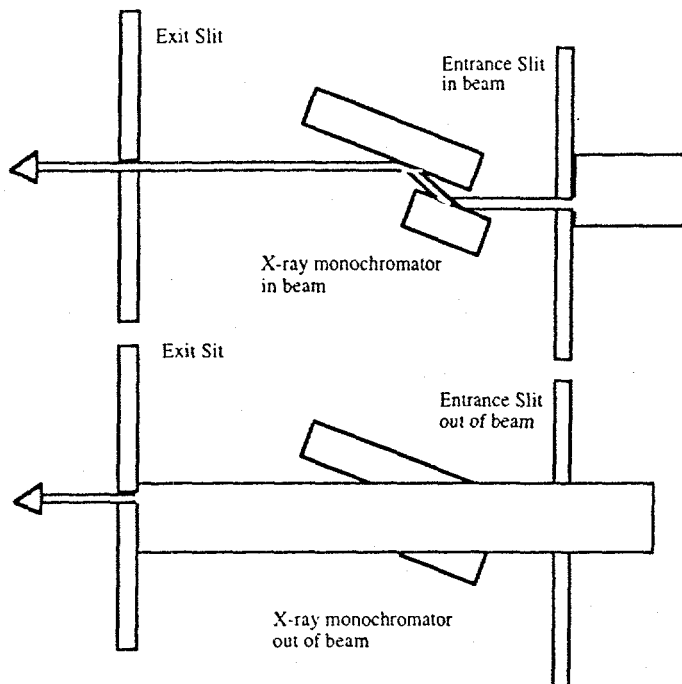


Fig. 4. A simple small displacement monochromator design. The exit slit ensures that the beam exits from the same vertical position regardless of whether it impinges directly on the slit or passed first through the monochromator. If the displacement and exit aperture are small compared to the incident beam dimension then the monochromator efficiently uses the available beam.

Alternatively, the angular 0.03 mrad difference between the direct beam and the monochromatic beam can be accommodated by heating the second crystal. The temperature difference, ΔT , required to tilt a Si (111) reflected beam 0.03 mrad depends on the x-ray energy; $\Delta T(\text{°C}) \equiv 2.5E$ (keV). A monochromator based on this concept is currently under construction by the Michigan-Howard University-Lucent collaborative access team (MHATT-Cat) at the APS.⁷

One consideration with even a 1 mm displacement is the change in the incident beam spectra. This may be an advantage or a disadvantage depending on the experiment. For example it is possible to move slightly away from the beam axis to increase the bandwidth of the undulator peaks. Alternatively the beam symmetrically above and below the beam centerline will have the same effective source size and beam spectra.

4-Crystal design

An alternative design uses 4 crystals with pairs of nondispersive crystals matched dispersively. This design has the advantage of eliminating all displacements and angular shifts between white and monochromatic beam operation (Fig. 5). One disadvantage with this design is a somewhat lower throughput due to the dispersive geometry. Because of the unusually high collimation of 3rd generation sources, the throughput of dispersive optics is much greater than for 2nd generation sources. The throughput at 20 keV is about 40% of a simple 2 crystal nondispersive design as shown in Fig. 6. A microdiffraction monochromator based on this principle is currently under development at the Advanced Light Source, ALS.⁸

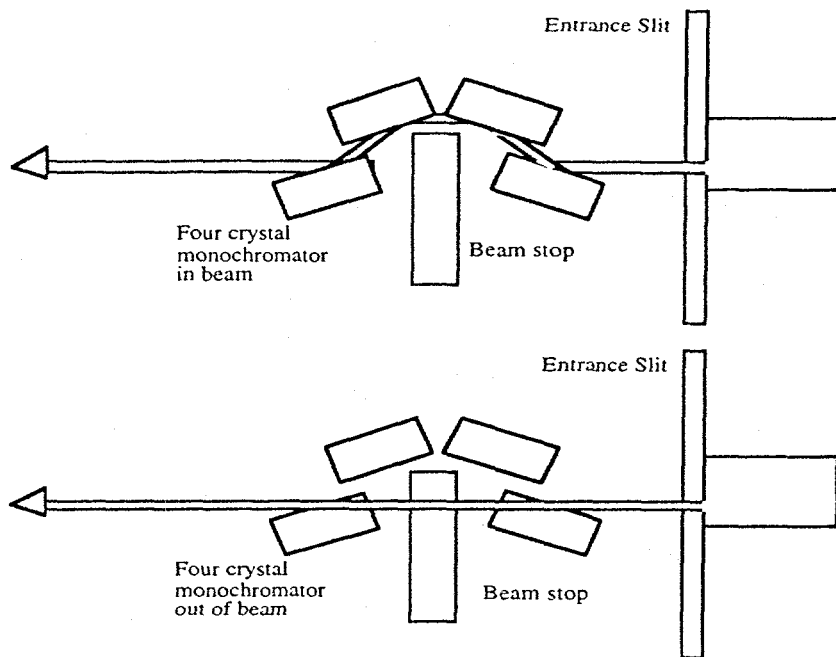


Fig. 5. Four crystal design with zero beam displacement.

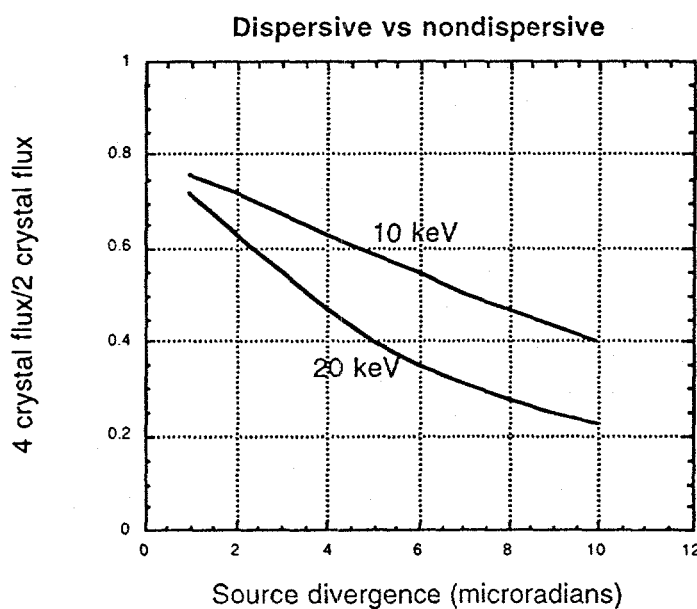


Fig. 6. Relative photon flux passed by a 2-crystal small displacement monochromator compared to a 4-crystal zero-displacement monochromator. The divergence from a high brilliance undulator on a third generation storage ring is on the order of $\sigma' \sim 5-10 \mu\text{rad}$. The divergence of a second generation storage ring is on the order of $100 \mu\text{rad}$.

3. FIRST CRYSTAL THERMAL PERFORMANCE

First crystal with water cooling

Variation in 2d

With either the 2 or 4 crystal designs, the first crystal must tolerate $\sim 1\text{-}4$ watts (Fig. 1) in an x-ray beam with a cross section of $\sim 0.03 \text{ mm}^2$ ($\sim 60 \text{ watts/mm}^2$). We have studied the thermal distortions introduced on a simple monolithic Si crystal under such a heat load. The thermal distortions were studied with various cooling geometries (side, back, etc.) with different distances from the end of the crystal, at different diffraction angles and with various beam sizes. At normal incidence (worst case), with 2 watts of power and simple back cooling, the temperature rise at the center of incident beam intercept is about 37°K . However, at the minimum design energy of 8 keV, the temperature rise is only about 10°K because the beam is spread over a four times larger surface area. If we assume a thermal expansion coefficient of $\sim 2.3 \times 10^{-6}$, then the d spacings of the crystal can vary by as much as $\Delta d/d \sim 2.3 \times 10^{-5}$. At 8 keV this corresponds to a range of $6 \mu\text{rad}$ in the monochromator tilt angles to maximize the diffraction efficiency for all parts of the monochromator crystal. However, the temperature variation over the illuminated footprint of the crystal is about five times smaller than the total thermal rise so that the effect of changes in the d spacing are expected to be small ($\sim 1 \mu\text{rad}$ worst case). As the x-ray energy increases, the footprint of the beam on the crystal increases which lowers the temperature rise for a given incident x-ray power. In addition, the angular tilt required to optimize the crystal bandpass for a given Δd also decreases with decreasing Bragg angle.

Longitudinal slope errors

The major effect of the thermal gradient on the crystal is a bump at the beam intercept which causes a variation of slopes across the beam intercept. A typical bump profile and slope errors are illustrated in Fig. 7a,b for a 2 watt beam spread over 2.4 mm. As can be seen in Fig. 7b, there is an almost purely cylindrical region in the center of the bump surrounded by discontinuities at the ends. The detailed shape of the thermal bump depends somewhat on the cooling geometry and the proximity to the end of the crystal, but the thermal bump has a character roughly as shown in Fig. 7 for most reasonable geometries.

The slope-change per unit length can be controlled by increasing the total illuminated footprint on the crystal. Increasing the footprint, moves the thermal discontinuities away from the center of the footprint. Fig. 8a plots the slope change/mm as a function of illuminated crystal length for a fixed power/unit length. Here the crystal is cooled on all four side surfaces but is not back cooled. Although the power absorbed by the crystal increases with longer illuminated footprints, the change in slope/mm at the center of the crystal decreases dramatically with length. This is very similar to the behavior observed in models of high-heat-load x-ray mirrors. With more careful modeling it may be possible to side cool the crystal to make the slope-change per unit length even smaller at the center of the illuminated footprint.

The details of the thermal bump depend on factors such as heat flux (Fig. 1), Bragg angle, and cooling geometry. As an example, we estimate the performance of a water cooled Si crystal at 10, 16 and 21 keV to anticipated performance of the crystal monochromator. At 10 keV, the power in a $0.3 \times 0.1 \text{ mm}$ beam is about 1.4 watts and the beam is spread over a 1.5mm long footprint on the first crystal. If we allow a slightly larger beam (0.48 mm high, 2.2 watts) to strike the crystal, then the thermal slope variation over the central 1.5 mm is about $8 \mu\text{rad}$ ($R=187 \text{ m}$) and the root-mean-square (RMS) slope variation is about $2.4 \mu\text{rad}$. For a random slope pattern this would result in an approximately 30% loss of beam brilliance. However, since as seen in Fig. 7b the slope variation is well correlated with longitudinal position along the crystal and has a nearly cylindrical shape, the crystal acts like a convex mirror. The $\pm 4 \mu\text{rad}$ tilt of the crystal planes corresponds to an approximately 13% bandpass mismatch between the extreme rays at 10 keV. Overall the two crystal monochromator should operate with good x-ray reflectivity and with negligible effect on beam brilliance.

At 21 keV, which is a good energy for x-ray microdiffraction, the situation is even better than at 10 keV. The beam power through a $0.1 \times 0.3 \text{ mm}^2$ aperture is about 2.4 watts, but the long wavelength first

harmonic can be removed with a low Z filter to yield a total power of about 1.5 watts spread over a 3.2mm footprint. Again it is best to allow a slightly larger beam to illuminate the first crystal to reduce the slope errors for the central portion of the illuminated footprint. For example, with an ~ 0.48 mm high beam (2.4 watts, 5mm footprint), the longitudinal slope variation over the central 3.2 mm is $\sim 6 \mu\text{rad}$ and the RMS slope variation is $\sim 1.7 \mu\text{rad}$. This should cause about a 20% loss of throughput for the extreme rays with a negligible effect on beam brilliance.

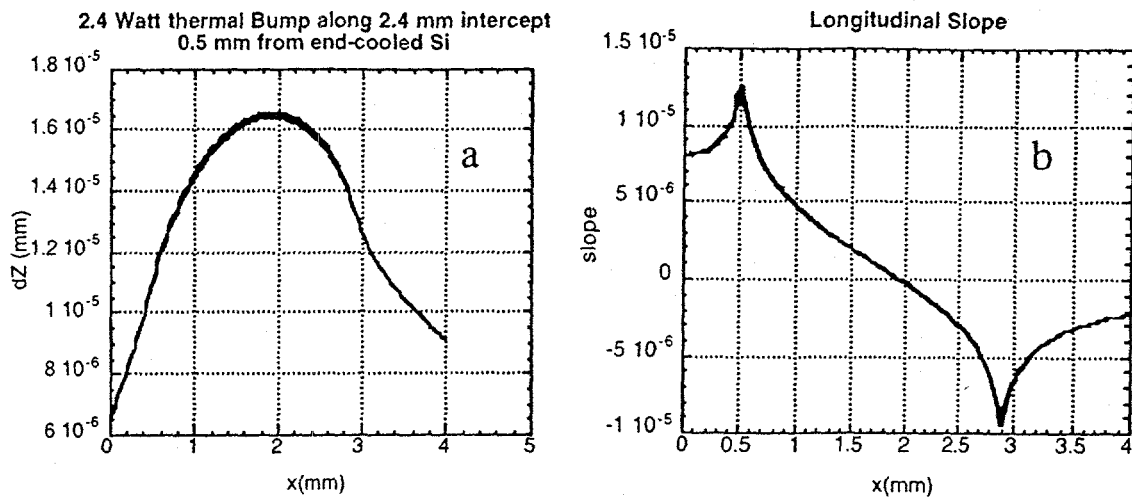


Fig 7 (a) Thermal bump on a Si(111) crystal with a 2 watt beam spread over a 2.4 mm long footprint 0.5 mm from the end of the crystal. Note that this figure has 6 traces along the length of the crystal each spaced horizontally 0.01 mm from the intercept centerline. (b) Slope of crystal surface.

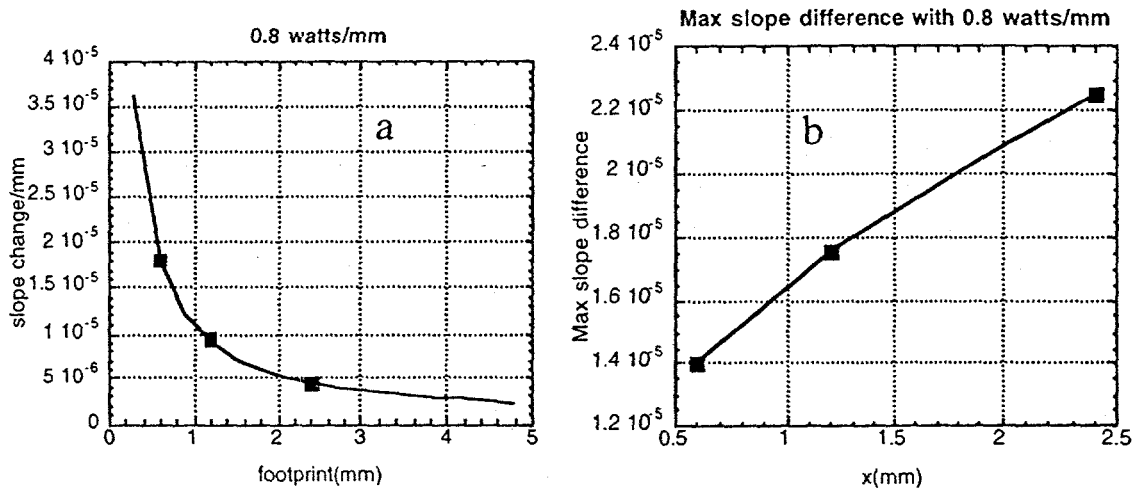


Fig. 8 (a) Change in slope/mm as a function of footprint length, at the center of a Si crystal with an absorbed power of 0.8 watts/mm in a 0.1mm wide beam (b) Maximum slope variation as a function of footprint length along a Si crystal with an absorbed power of 0.8 watts/mm in a 0.1mm wide beam.

Below 8 keV and in an intermediate range between ~ 11 and 16 keV, the thermal distortions introduced on the first crystal may be unacceptable with simple water cooling. At 16 keV for example, the total power

through the $0.1 \times 0.3 \text{ mm}^2$ aperture is about 3.2 watts. Low Z filtering can reduce this power to about 2.8 watts. We assume again that the crystal intercepts a 0.48 mm high beam and that only the central 0.3 mm footprint is passed through the final aperture. The estimated slope variation across the central 2.4 mm footprint is $10 \mu\text{rad}$ with an RMS tilt variation of $3 \mu\text{rad}$. The loss of throughput for the extreme rays is about 26% for an overall flux loss of about 13%. For random slope errors with an RMS of $3 \mu\text{rad}$, the loss in brilliance is about 45%. Again, because the slope variation is small and almost linear over the central 2.4 mm of the crystal, the effective brilliance loss may actually be small.

Sagittal slope errors

Sagittal slope errors across the 0.1mm wide beam are negligible for all cases studied. Sagittal errors are particularly small because the beam brilliance is lower in the horizontal plane and because sagittal slope errors cause smaller beam tilts compared with longitudinal slope errors.

Thin Crystal Geometry:

The power absorbed by the monochromator can be further reduced by the use of a thin crystal concept as discussed by Knapp et al.³ Typically a Si crystal of about 0.6mm thickness absorbs only half of the incident beam power. We estimate the beam power absorbed in a thin Si crystal with a carbon prefilter. As illustrated in Fig. 9, a thin crystal transmits about half of the incident power up to 0.4mm at 10 keV. At 20 keV a 0.6mm thick crystal transmits about half the incident power. Preliminary modeling however indicates that thin crystals do not work as well as thick crystals with water cooling.

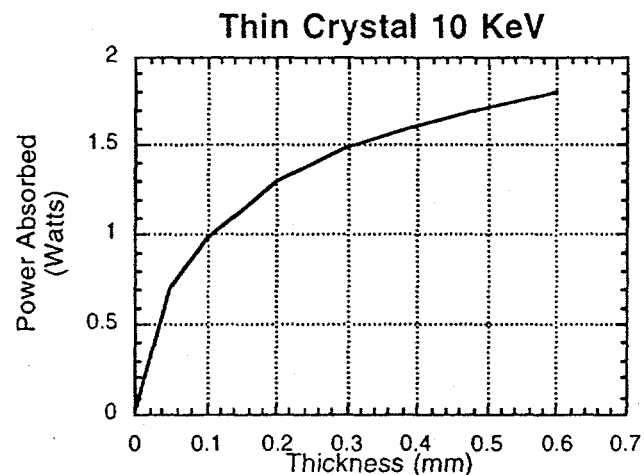


Fig. 9 Power absorbed by a thin Si (111) crystal as a function of the crystal thickness when set to diffract at 10 keV. The incident beam is assumed to be $0.1 \times 0.3 \text{ mm}$ in area.

First crystal with liquid N₂ cooling

Even better performance is possible if the crystal is cooled to liquid N₂ temperatures. Because only a few watts of power are absorbed by the first crystal, a simple copper braid connected to a liquid N₂ bath can be used to cool the first Si crystal to a region of near zero thermal expansion coefficient and greater thermal conductivity. The combination of better thermal conductivity and lower thermal expansion will allow the small crystal designs to be easily extended to 200 or 300 mA operations.

4. CONCLUSION

Only small beams are required for experiments such as coherent scattering and x-ray microdiffraction. The distortions modeled for a water cooled first Si (111) crystal intercepting an $\sim 0.03 \text{ mm}^2$ x-ray beam with ~ 2 watts of power are relatively small and do not degrade beam brilliance. It appears that for small cross section beams, a simple water cooled crystal can tolerate the high thermal density from an APS type A undulator operating at 100mA. Best performance is in the energy range between 8-10 keV and 16-22 keV where power densities are lowest. Liquid N₂ cooling through a copper braid can extend the small crystal design to 300 mA operation and can allow operation from 4-22 keV.

5. ACKNOWLEDGMENT

Research sponsored in part by the Laboratory Directed Research and Development Program of the Oak Ridge National Laboratory and the Division of Material Sciences, U.S. Department of Energy under contract DE-AC05-96OR22464 with Lockheed Martin Energy Research Corporation and by the U.S. Department of Energy BES Materials Science under Contract No. W-31-109-ENG-38.

6. REFERENCES

1. A. M. Khounsary, *Rev. Sci. Instrum.* **63** 461 (1992).
2. L.E. Berman, J.B. Hastings, D.P. Siddons, M. Koike, V. Stojanoff and M. Hart, *Nuc. Inst. and Meth. A* **329** 555 (1993).
3. G.S. Knapp, C.S. Rogers, M.A. Beno, C.L. Wiley, G. Jennings, and P.L. Cowan, *Rev. Sci. Instrum.* **66** 2138 (1995).
4. G.E. Ice, "Microbeam-Forming Methods for Synchrotron Radiation", *X-ray Spectrometry*, accepted for publication.
5. G.E. Ice, *Nuc. Instr. and Meth. B* **24/25** 397 (1987).
6. R. Rebonato, G.E. Ice, A. Habenschuss, and J.C. Billelo, *Phil. Mag. A* **60** 571 (1989).
7. W. Lowe, MHATT-CAT, Howard University, Washington DC, private communication.
8. A. Thompson, ALS, Lawrence Berkeley National Laboratory, Berkeley CA, private communication.
9. M. Marcus, et al. *Proceedings Spring MRS meeting San Francisco CA* to be published.